

***p*-type ZnO films with solid-source phosphorus doping by molecular-beam epitaxy**

F. X. Xiu, Z. Yang, L. J. Mandalapu, and J. L. Liu^{a)}

Quantum Structures Laboratory, Department of Electrical Engineering, University of California, Riverside, California 92521

W. P. Beyermann

Department of Physics, University of California, Riverside, California 92521

(Received 8 August 2005; accepted 7 December 2005; published online 31 January 2006)

Phosphorus-doped *p*-type ZnO films were grown on *r*-plane sapphire substrates using molecular-beam epitaxy with a solid-source GaP effusion cell. X-ray diffraction spectra and reflection high-energy electron diffraction patterns indicate that high-quality single crystalline (11 $\bar{2}$ 0) ZnO films were obtained. Hall and resistivity measurements show that the phosphorus-doped ZnO films have high hole concentrations and low resistivities at room temperature. Photoluminescence (PL) measurements at 8 K reveal a dominant acceptor-bound exciton emission with an energy of 3.317 eV. The acceptor energy level of the phosphorus dopant is estimated to be 0.18 eV above the valence band from PL spectra, which is also consistent with the temperature dependence of PL measurements. © 2006 American Institute of Physics. [DOI: 10.1063/1.2170406]

With a wide band gap of 3.37 eV and a large exciton binding energy of 60 meV at RT, ZnO has attracted tremendous interests for developing highly efficient optoelectronic devices.¹ However, making a reliable and reproducible *p*-type ZnO film is still a bottleneck. The difficulty mainly arises from the self-compensating effect of native defects (V_o and Zn_i) (Ref. 2) and/or hydrogen incorporation.³

In recent years, different kinds of dopants, such as group V elements nitrogen,^{4–10} phosphorous,^{11–14} arsenic,^{15–18} and antimony,^{19–21} have been employed to achieve *p*-type ZnO films. Among them, phosphorus-doped ZnO films exhibited high carrier concentrations, reasonable mobilities, and low resistivities.^{11,13} However, there are several challenges on current *p*-type ZnO films via phosphorus doping. First, the phosphorus-doped ZnO films were mainly grown by pulsed laser deposition¹² and radio-frequency sputtering methods.¹³ Unlike molecular-beam epitaxy (MBE) or chemical vapor deposition, high-quality single crystalline ZnO films are difficult to obtain. Second, the dopant source in the film, for example P₂O₅, must be thermally dissociated in order to provide the phosphorus dopants after growth. Unfortunately, this process largely depends on rapid thermal annealing conditions and may yield unreliable *p*-type conduction. Third, some phosphorus-based compounds that are currently being used, such as Zn₃P₂, are undesirable because they are toxic.

In our study, we used a solid-source GaP effusion cell in an SVTA MBE system. A special design of Ga-trapping-cap system, which included a dome-shaped and a disk-shaped pyrolytic-boron-nitride (PBN) extension cap on top of a PBN crucible, was employed with this effusion cell. Upon decomposition of the GaP compound at high temperatures (P₂ and parasitic Ga atoms), all Ga atoms would strike the caps at least once and are trapped in the cap region where the temperature is lower than that inside the crucible. As a result, a P₂ dominated beam is obtained. The simplicity of the GaP

effusion cell design and the good controllability of P₂ beam²² make this doping technique an advantageous alternative for ZnO *p*-type doping.

p-type phosphorus-doped ZnO films were grown on (01 $\bar{1}$ 2) *r*-plane sapphire substrates. Elemental zinc (5N) was evaporated with a low-temperature (LT) effusion cell. The oxygen (5N) plasma was generated with a radio-frequency plasma source. Prior to growth, several cleaning procedures were followed. First, substrates were dipped into an aqua regia solution (HCL:HNO₃=3:1) at 100 °C for 30 min to remove surface contaminants and scratches, and then they were dried with nitrogen gas. Second, the substrates were transferred into the growth chamber and annealed under vacuum at 800 °C for 20 min. After thermal annealing, an oxygen plasma treatment was performed at 720 °C for 15 min to generate an oxygen-terminated surface.²³ Finally, undoped and phosphorus-doped ZnO films were grown at 720 °C. Different GaP cell temperatures were employed for the phosphorus-doped ZnO growth. At the end of growth, annealing was carried out at 800 °C for 20 min to activate the phosphorus dopants,¹³ followed by *in situ* reflection high-energy electron diffraction (RHEED) observations of the films.

The crystal structure and orientation of ZnO films were investigated using a Bruker advanced D8 x-ray diffractometer. X-ray diffraction (XRD) θ -2 θ spectra for the undoped and phosphorus-doped ZnO films are shown in Figs. 1(a)–1(c). The *r*-plane sapphire substrates exhibit two peaks at 25.8° and 52.8°, corresponding to (01 $\bar{1}$ 2) and (02 $\bar{2}$ 4), respectively.²⁴ ZnO, however, shows a sharp peak at 56.7°, indicating a single crystalline film with a (11 $\bar{2}$ 0) plane grown on the substrate. The full width at half maximum (FWHM) values of 5.3, 30.2, and 37.0 arc min were obtained for samples A, B, and C, respectively. The dramatic increase of the FWHM values indicates the incorporation of phosphorus into the films. The insets of Fig. 1 are *in situ* RHEED patterns at the end of film growth. For the undoped and lightly phosphorus-doped ZnO films, RHEED patterns are sharp and

^{a)} Author to whom correspondence should be addressed; electronic mail: jianlin@ee.ucr.edu

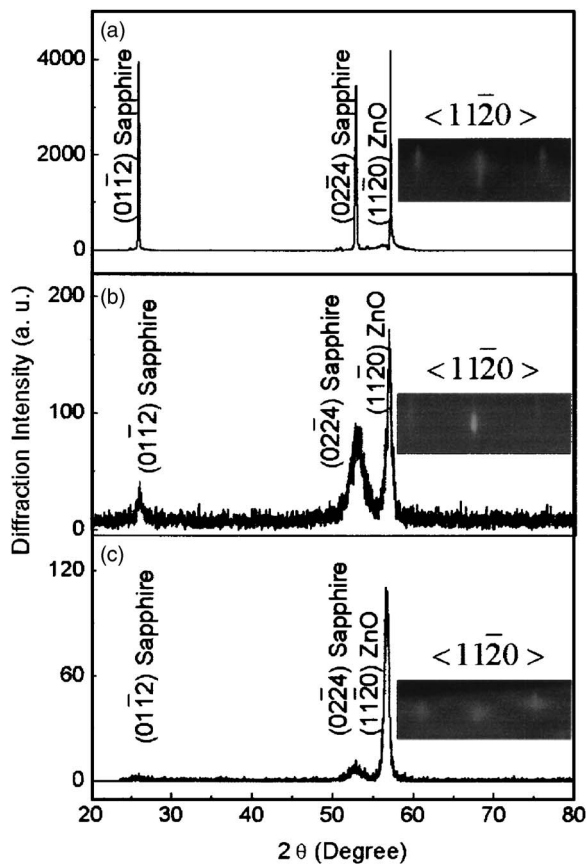


FIG. 1. (Color online) XRD spectra and RHEED patterns (inset) for (a) undoped ZnO (sample A), (b) phosphorus-doped ZnO with a GaP cell temperature of 710 °C (sample B), and (c) phosphorus-doped ZnO with a GaP cell temperature of 750 °C (sample C).

streaky, showing a two-dimensional growth mode. The orientations can be identified as $\langle 11\bar{2}0 \rangle$.²⁴ By raising the GaP cell temperature to 750 °C, however, a spotty RHEED pattern was observed, demonstrating a three-dimensional growth mode occurred.

Hall and resistivity measurements were carried out to characterize the electrical properties of all ZnO films with a physical property measurement system. Figure 2 shows the Hall resistance R_{Hall} as a function of magnetic field at RT for sample B; the positive slope, which is Hall coefficient, indicates p -type conduction. The inset shows a typical I - V curve for sample B. The linear characteristic indicates that good Ti/Al Ohmic contacts were achieved.

The results of RT Hall and resistivity measurements for both undoped and phosphorus-doped ZnO samples are summarized in Table I. The undoped ZnO film has an n -type conductivity with an electron concentration of $1.0 \times 10^{17} \text{ cm}^{-3}$ and a mobility of $46.5 \text{ cm}^2/\text{V s}$. The phosphorus-doped ZnO films, however, show strong p -type conductivities. With a relatively low GaP cell temperature of

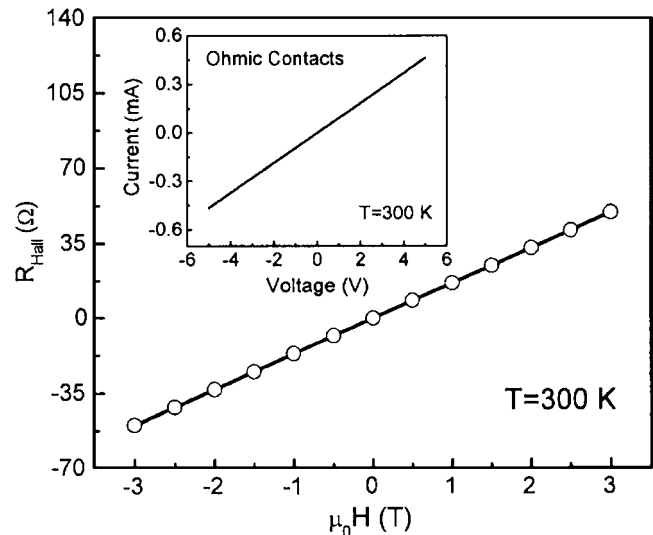


FIG. 2. The Hall resistance as a function of applied magnetic field at RT for a phosphorus-doped ZnO film (sample B). The inset is a I - V curve for this sample.

710 °C (sample B), the film exhibits a hole concentration of $1.2 \times 10^{18} \text{ cm}^{-3}$ and a mobility of $4.2 \text{ cm}^2/\text{V s}$. By raising the cell temperature to 750 °C (sample C), the hole concentration increases to $6.0 \times 10^{18} \text{ cm}^{-3}$, and the mobility decreases to $1.5 \text{ cm}^2/\text{V s}$. Figure 3 shows the temperature dependence of the hole concentration for a phosphorus-doped ZnO film (sample B). The carrier concentration decreases at lower temperature as a result of carrier freeze-out. The inset shows the Hall mobility as a function of temperature. From 250 to 350 K, the Hall mobility is dominated by phonon scattering while below 120 K ionized impurity scattering takes over. In between 120 and 250 K, the two mechanisms coexist. Table I also shows the resistivity values for different films. With a GaP cell temperature of 750 °C, sample C exhibits a low resistivity of $0.7 \text{ } \Omega \text{ cm}$, which is comparable to the value reported for phosphorus-doped ZnO films with P_2O_5 as the dopant.¹³

LT PL measurements were performed to characterize the optical excitations of undoped and phosphorus-doped ZnO films. Figure 4(a) shows a spectrum for the undoped ZnO film (sample A) measured at 8 K. A strong near-band edge emission associated with the neutral-donor-bound exciton ($D^\circ X$) is observed at 3.366 eV. For the lightly doped ZnO film (sample B), however, a new peak at 3.315 eV is observed besides the $D^\circ X$ emission at 3.364 eV, as shown in Fig. 4(b). The PL spectrum in Fig. 4(c) is completely dominated by a strong peak at 3.317 eV with a weak $D^\circ X$ emission at 3.360 eV for the heavily doped ZnO film (sample C). From the evolution of PL spectra, it can be inferred that the peak at 3.317 eV is the neutral-acceptor-bound exciton ($A^\circ X$) emission, resulting from phosphorus doping. The other peaks at 3.258 and 3.179 eV in Fig. 4(c) are assigned to

TABLE I. Electrical properties of undoped and phosphorus-doped ZnO films at RT.

Sample	GaP cell temp. (°C)	Type	Film thickness (μm)	Mobility ($\text{cm}^2/\text{V s}$)	Resistivity ($\Omega \text{ cm}$)	Carrier density (cm^{-3})
A	Undoped	n	0.5	46.5	1.3	1.0×10^{17}
B	710	p	0.2	4.2	1.2	1.2×10^{18}
C	750	p	0.2	1.5	0.7	6.0×10^{18}

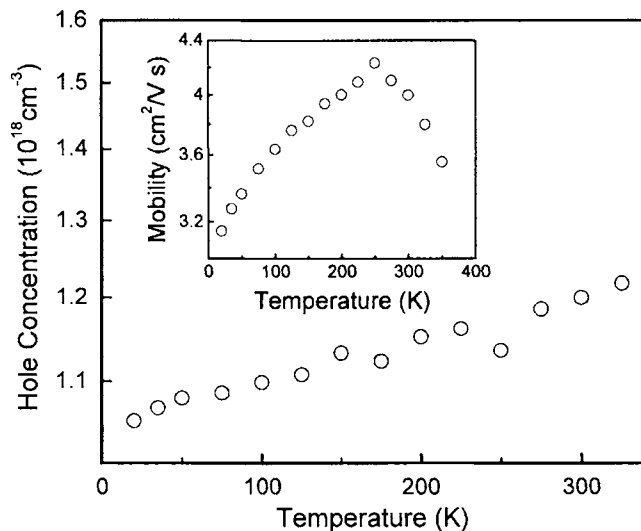


FIG. 3. Temperature dependence of the hole concentration for a phosphorus-doped ZnO film (sample B). The inset shows Hall mobility as a function of temperature (sample B).

be free electron to acceptor level (FA) and donor-acceptor pair (DAP) transitions, respectively. The binding energy of an acceptor E_A can be calculated with¹⁵

$$E_A = E_{\text{gap}} - E_{\text{FA}} + k_B T/2, \quad (1)$$

where E_{FA} is the temperature-dependent transition. With an intrinsic band gap of $E_{\text{gap}} = 3.437$ eV,^{7,11,15} the value of E_A is then calculated to be 0.18 eV.

PL measurements were performed on the phosphorus-doped ZnO film (sample B) at temperatures ranging from 8 to 300 K, as shown in Fig. 4(d). The inset shows the energy-integrated intensity of the $A^\circ X$ emission as a function of temperature. By fitting the intensity and combining the Haynes rule, an acceptor activation energy E_A is calculated to

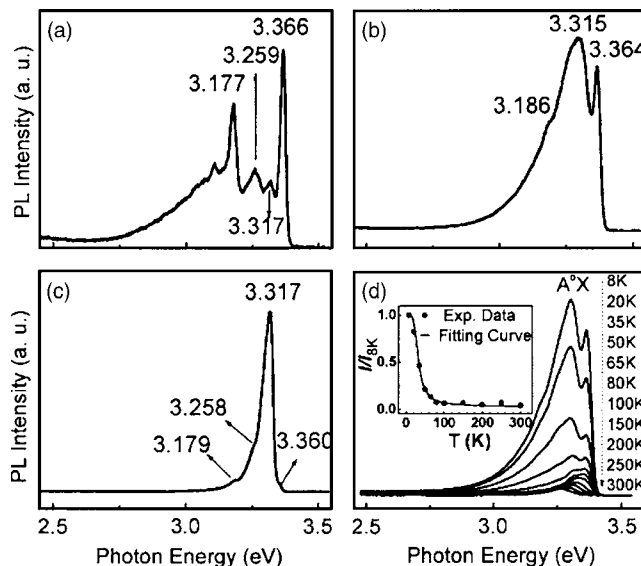


FIG. 4. PL spectra measured at $T=8$ K for (a) undoped ZnO (sample A), (b) phosphorus-doped ZnO with a GaP cell temperature of 710 °C (sample B), and (c) phosphorus-doped ZnO with a GaP cell temperature of 750 °C (sample C); (d) shows the PL spectra measured for several temperatures over the range from 8 to 300 K (sample B). The inset shows the energy-integrated intensity of the $A^\circ X$ emission as a function of temperature. The dots represent the experimental data, and the solid line is the fit.

be 172 meV. This result is in good agreement with the value for the acceptor activation energy of 0.18 eV obtained from spectroscopic data using Eq. (1).

In summary, high-quality p -type phosphorus-doped ZnO films were produced using a GaP effusion cell as a phosphorus dopant source in a MBE system. Hall and resistivity measurements reveal that phosphorus-doped ZnO films exhibit p -type conductivities. A carrier concentration of $6.0 \times 10^{18} \text{ cm}^{-3}$, Hall mobility of $1.5 \text{ cm}^2/\text{V s}$, and resistivity of $0.7 \text{ } \Omega \text{ cm}$ were measured in a phosphorus-doped ZnO film. LT PL spectra reveal a strong peak at 3.317 eV, which was attributed to the phosphorus-associated $A^\circ X$ emission, and from these data the activation energy of phosphorus impurities is estimated to be 0.18 eV. This conclusion is consistent with the temperature dependence of PL emission spectra.

This work was supported by DARPA/DMEA through the center for NanoScience and Innovation for Defense (CNID) under Award No. H94003-04-2-0404. The authors would like to acknowledge Joo-Young Lee (at UCLA, EE department) for RT Hall measurements.

- ¹D. C. Look and B. Claflin, Phys. Status Solidi B **241**, 624 (2004).
- ²S. B. Zhang, S. H. Wei, and A. Zunger, Phys. Rev. B **63**, 075205 (2001).
- ³C. G. Van de Walle, Phys. Rev. Lett. **85**, 1012 (2000).
- ⁴A. Tsukazaki, A. Ohtomo, T. Onuma, M. Ohtani, T. Makino, M. Sumiya, K. Ohtani, S. F. Chichibu, S. Fuke, Y. Segawa, H. Ohno, H. Koinuma, and M. Kawasaki, Nat. Mater. **4**, 42 (2005).
- ⁵J. M. Bian, X. M. Li, C. Y. Zhang, W. D. Yu, and X. D. Gao, Appl. Phys. Lett. **85**, 4070 (2004).
- ⁶D. C. Look, D. C. Reynolds, C. W. Litton, R. L. Jones, D. B. Eason, and G. Cantwell, Appl. Phys. Lett. **81**, 1830 (2002).
- ⁷H. W. Liang, Y. M. Lu, D. Z. Shen, Y. C. Liu, J. F. Yan, C. X. Shan, B. H. Liu, Z. Z. Zhang, J. Y. Zhang, and X. W. Fan, Phys. Status Solidi A **202**, 1060 (2005).
- ⁸J. G. Lu, Z. Z. Ye, F. Zhuge, Y. J. Zeng, B. H. Zhao, and L. P. Zhu, Appl. Phys. Lett. **85**, 3134 (2004).
- ⁹E. Kamiska, A. Piotrowska, J. Kossut, R. Butkut, W. Dobrowolski, R. ukasiewicz, A. Barcz, R. Jakiela, E. Dynowska, E. Przedziecka, M. Aleszkiewicz, P. Wojnar, and E. Kowalczyk, Phys. Status Solidi C **2**, 1119 (2005).
- ¹⁰X. Li, Y. Yan, T. A. Gessert, C. L. Perkins, D. Young, C. DeHart, M. Young, and T. J. Coutts, J. Vac. Sci. Technol. A **21**, 1342 (2003).
- ¹¹D. K. Hwang, H. S. Kim, J. H. Lim, J. Y. Oh, J. H. Yang, S. J. Park, K. K. Kim, D. C. Look, and Y. S. Park, Appl. Phys. Lett. **86**, 151917 (2005).
- ¹²V. Vaithianathan, B. T. Lee, and S. S. Kim, Phys. Status Solidi A **201**, 2837 (2004).
- ¹³K. K. Kim, H. S. Kim, D. K. Hwang, J. H. Lim, and S. J. Park, Appl. Phys. Lett. **83**, 63 (2003).
- ¹⁴Z. Q. Chen, A. Kawasuso, Y. Xu, H. Naramoto, X. L. Yuan, T. Sekiguchi, R. Suzuki, and T. Ohdaira, J. Appl. Phys. **97**, 013528 (2005).
- ¹⁵Y. R. Ryu, T. S. Lee, and H. W. White, Appl. Phys. Lett. **83**, 87 (2003).
- ¹⁶D. C. Look, G. M. Renlund, R. H. Burgener II, and J. R. Sizelove, Appl. Phys. Lett. **85**, 5269 (2004).
- ¹⁷V. Vaithianathan, B. T. Lee, and S. S. Kim, Appl. Phys. Lett. **86**, 062101 (2005).
- ¹⁸T. S. Jeong, M. S. Han, C. J. Youn, and Y. S. Park, J. Appl. Phys. **96**, 175 (2004).
- ¹⁹T. Aoki, Y. Shimizu, A. Miyake, A. Nakamura, Y. Nakanishi, and Y. Hatanaka, Phys. Status Solidi B **229**, 911 (2002).
- ²⁰F. X. Xiu, Z. Yang, L. J. Mandalapu, D. T. Zhao, J. L. Liu, and W. P. Beyermann, Appl. Phys. Lett. **87**, 152101 (2005).
- ²¹F. X. Xiu, Z. Yang, L. J. Mandalapu, D. T. Zhao, and J. L. Liu, Appl. Phys. Lett. **87**, 252102 (2005).
- ²²T. Shitara and K. Eberl, Appl. Phys. Lett. **65**, 356 (1994).
- ²³Y. F. Chen, D. M. Bagnall, H. J. Koh, K. T. Park, K. Hiraga, Z. Q. Zhu, and T. Yao, J. Appl. Phys. **84**, 3912 (1998).
- ²⁴C. R. Gorla, N. W. Emanetoglu, S. Liang, W. E. Mayo, Y. Lu, M. Wra-back, and H. Shen, J. Appl. Phys. **85**, 2595 (1999).